Microchemical Journal 147 (2019) 643–653

Contents lists available at ScienceDirect

Microchemical Journal

journal homepage: www.elsevier.com/locate/microc

Photocatalytic degradation of catechol using ZnO nanoparticles as catalyst: Optimizing the experimental parameters using the Box-Behnken statistical methodology and kinetic studies

Edris Bazrafshan[a], Tariq J. Al-Musawi[b], Marcela Fernandes Silva[c], Ayat Hossein Panahi[d,*], Mohammad Havangi[e], Ferdos Kord Mostafapur[e]

[a] Health Sciences Research Center, Torbat Heydariyeh University of Medical Sciences, Torbat Heydariyeh, Iran
[b] Isra University, Department of Civil Engineering, Amman, Jordan
[c] Chemical Engineering Department, Universidade Estadual de Maringà, Av. Colombo n°5790, CEP 87020-200 Maringà, PR, Brazil
[d] Social Determinants of Health Research Center, Birjand University of Medical Sciences, Birjand, Iran
[e] Environmental Health, Faculty of Health, Zahedan University of Medical Sciences, Zahedan, Iran

ARTICLE INFO

Keywords:
Catechol
ZnO nanoparticles
Photocatalytic
Environmental parameters
Optimization
Box-Behnken methodology

ABSTRACT

A catalyst of ZnO nanoparticles was used in the photocatalytic process of treatment for potential use towards catechol degradation in an aqueous solution. The investigation of the characterization was carried out using TEM, SEM, XRD, and FT-IR techniques, which indicated that the catalyst of ZnO nanoparticles possesses unique catalytical features related to the surface morphology, structure, and functional groups. The efficiency of degradation was put to the test in relation to the variation of several experimental parameters including: pH (3–11); dose nanoparticles (0.2–0.25 g/L); reaction time (15–120 min); initial concentration (10–200 mg/L), and intensity of UV radiation (8–40 W). These aforementioned parameters were optimized and examined for the influence that they exerted on the efficiency of degradation which involved the usage of the Box-Behnken design methodology. According to the ANOVA results that yielded a confidence level of 95%, a high regression along with fitting values were obtained between the results of the experimental degradation of catechol and the predicted quadratic model. The kinetic study revealed that the data on experimental degradation could be described by using the Langmuir-Hinshelwood expression, which showed high precision values of the coefficient of regression. The optimum efficiency of degradation of 69.8% was achieved at optimized experimental conditions of pH = 3, a dosage of ZnO nanoparticles equal to 0.24 g/L, a reaction time of 98 min, with an initial concentration of catechol of 74 mg/L, and with the intensity of UV radiation equal to 40 W. Thus, the present study indicated that a catalyst of ZnO nanoparticles has a high practical utility, and exhibits good performance as a catalyst for degradation of catechol in a photocatalytic process.

1. Introduction

Environmental hazards relating to the pollution of global water resources as a result of discharge of several hazardous phenolic compounds has been proved to be a critical and life-threatening issue in many countries, especially when these water resources were the only available sources of drinking water for the population. This dangerous situation is caused by organic chemicals that have a high affinity towards transforming into carcinogenic disinfection byproducts, especially during the process of chlorination of water or wastewater [1–4]. Furthermore, color, taste, and odor are the three most common problems that are caused by high concentrations of organic matters such as phenols in water [5–8]. Moreover, heavy metals, which are known to be dangerous and carcinogenic, may combine with the organic matter present in water leading to their transportation and mixing into the water resources. Besides these drawbacks, the organic material itself may form biofilms within the water distribution network pipelines [9].

Catechol (1,2-Dihydroxybenzene) is one among the most highly toxic phenolic compounds, which is used as an antiseptic. This compound also has the ability to enter the paper, photography, and leather industries [10–12]. Furthermore, catechol compounds have been detected in elevated concentrations in the effluents from petrochemical refineries, steel mills, and pharmaceutical factories. The metabolism that human bodies undergo owing to acute or chronic catechol

* Corresponding author.
E-mail addresses: tariqjwad@yahoo.com (T.J. Al-Musawi), ayatpanahi@yahoo.com (A.H. Panahi).

https://doi.org/10.1016/j.microc.2019.03.078
Received 18 December 2018; Received in revised form 4 March 2019; Accepted 25 March 2019
Available online 26 March 2019
0026-265X/

exposure can cause several serious health issues, like: irritation of the eyes and skin; neurological and respiratory tract diseases; genetic mutation; and have even been known to result in death in some cases [10,13]. According to the US EPA and WHO standards, the maximum allowable concentration of phenol and the compounds of its subclasses contained in industrial wastewater effluents and drinking water should not exceed 1 mg/L and 0.1 μg/L, respectively [13–18].

Various advanced methods of water treatment were suggested for elimination and degradation of phenolic compounds from wastewater prior to being discharged in the aquatic environment [19,20]. Among such methods, adsorption; electrocoagulation; biodegradation; membrane techniques; and advanced oxidation processes, have been extensively applied for this purpose [13,21–23]. The photocatalytic process is one of the advanced oxidation processes that is currently widely used in the tertiary treatment units for the degradation of a wide range of organic matter that is loaded in wastewater. The basis of this process involves the application of UV radiation for the production and reaction of free radicals hydroxyl as an oxidant agent with the presence of metal oxide ions as a metal catalyst (semiconductors) to produce the strong degradation agent, OH· [24–27]. The final products of these processes are water and CO_2 gas [12,13]. Recently, several natural and artificial low cost materials were applied as a metal catalyst [28,29]. Indeed, the science of nanotechnology opened new avenues in many engineering fields, especially in the synthesizing and utilization of nanoparticles as a catalyst to break up hazardous pollutants that get loaded into water and wastewater. For example, ZnO nanoparticles are one of the most frequently suggested nanomaterials to be employed as a catalyst in photocatalytic reactions. The main advantages of ZnO nanoparticles when compared with other catalyst materials include absorption of a wide spectrum of electromagnetic waves, availability, low cost, nonvolatility, lack of toxicity, capacity for high absorption, and have high chemical stability and reactivity [30,31]. In addition to all these, this material has an adjustable morphology and properties of chemical stability [20]. It is insoluble in water, therefore, surface morphology is controlled, particle size, and crystalline structure can be achieved [32,33]. Therefore, we speculated, which is the aim of this work, that ZnO nanoparticles could turn out to be a practical catalyst material for removal of catechol from any aquatic medium using the photocatalytic degradation method of treatment.

During the exposure of the semiconductors (ZnO nanoparticles in the present study) to UV radiation in the photocatalytic processes, the semiconductor photons get excited and their energy will be equal to, or greater than, the ground state. These excited electrons have a tendency to revert quickly to the ground state energy while simultaneously emitting photons. Ultimately, the photons emitted produce a radical hydroxyl which enhances the process of degradation of pollutants. The chemical reactions given by Eqs. (1) to (6) show the mechanism of this phenomenon [26].

$$ZnO + hv \rightarrow e_{cb}^{-} + h^{+} \quad (1)$$

$$ZnO\ (h^{+}) + OH \rightarrow OH^{\cdot} + ZnO \quad (2)$$

$$ZnO\ (e^{-}) + O_2 \rightarrow O_2^{\cdot} + ZnO \quad (3)$$

$$O_2^{\cdot} + H^{+} \rightarrow OOH^{\cdot} \quad (4)$$

$$OOH^{\cdot} + O^{\cdot -} + H^{+} \rightarrow O_2 + H_2O_2 \quad (5)$$

$$O^{\cdot -} + H_2O_2 \rightarrow OH^{\cdot} + OH^{+} + O_2 \quad (6)$$

Owing to the fact that the chemical and physical specifications of both catalyst particles and pollutant molecules vary significantly depending on the surrounding environment, leading to the investigation into the degradation of the efficiency of the pollutant in the photocatalytic process, this requires to be tested and optimized under different environmental conditions [34]. The Box-Behnken design methodology is the most commonly used method in the application of surface methodology response [35,36]. This advanced statistical tool was proved to be a popular, easy, and efficient expression design tool, which was put to practical use by several studies for modeling and optimizing the values of the process parameters [35,37,38]. This is owing to the fact that this methodology possesses several advantages as this technique is considered to be rapid and needs only a short duration of time to execute the optimization process compared with the other methods. Consequently, the number of experimental tests required identifying the degree of interaction of multiple factors and their effects in a system can be reduced. Normally, the Box-Behnken methodology (partly from Response Surface Methodologies) is applied when only a few experimental parameters are involved in the process [38,39].

On the basis of our knowledge, there have been none, or very few papers that have discussed using ZnO nanoparticles as a catalyst in a photocatalytic advanced oxidation process for the purpose of elimination of catechol from aqueous solutions. Besides, a limited number of studies have been conducted to examine the effects of optimization of the experimental parameters in this advanced method of treatment. Therefore, the present study was documented with the aim of investigating into the degradation efficiency of catechol using ZnO nanoparticles as a catalyst in a photocatalytic reactor. Additionally, the effects of several experimental parameters on the degradation efficiency of catechol were studied and optimized using the Box-Behnken experimental design methodology. The studied parameters are: pH; ZnO nanoparticles dose; reaction time; initial concentration; and intensity of UV radiation, where the highest and lowest limits of these parameters have been chosen depending on the limitations and conditions of most photocatalytic processes arising from the nature and properties of most of the water and wastewater in the environment [16,28,36,40].

2. Materials and methods

2.1. Chemicals and apparatus

A quantity of 0.5 kg analytical grade high purity catechol powder (chemical formula: $C_6H_4(OH)_2$; purity: ≥99%, with molecular weight of 110.11 g/mol) was purchased from Sigma-Aldrich (Germany). Further, the stock catechol solution (concentration of 1000 mg/L) was prepared in the laboratory by dilution of an appropriate amount of catechol powder with deionized water. Thereafter, all working solutions at the desired concentrations were also prepared via dilution of the stock solution by using deionized water. All the experimental samples were analyzed with the purpose of finding out the concentration of catechol by using spectrophotometric equipment (model LUV-100, Japan) at a wavelength of 285 nm. Additionally, the pH values were regulated throughout the experimental work by using 1.0 N of HCl and NaOH solutions by using a pH meter (Denver Instrument, Model: UB-10). The mixing process of the working solutions was carried out with the use of a magnetic shaker (model Alpha D500).

2.2. Catalyst characterization

The ZnO nanoparticles which were utilized as the metal catalyst material in the present study, was sourced from Sigma-Aldrich (USA) (particle size < 100 nm; surface area = 25 m^2/g; and pore volume range from 0.68 to 0.78 cm^3/g). The crystalline structure was examined by using an X-Ray diffractometer (XRD) (Model: D500, Siemens company, Germany), equipped with a high-power Cu Kα radiation source (1.54056 Å wavelength), that was generated at the rate of 40 kV/40 mA, in which all the XRD patterns of ZnO were collected in the 2θ range of 15° and 80°, with a step width of 0.02°, and a scan rate of 1°/s. A transmission electron microscopy (TEM) image was taken by using a Philips CM30 Scanning Transmission Electron Microscope (Philips CM30, The Netherlands). Also, a scanning electron microscopy (SEM) image was captured using a TESCAN BRNO-Mira3 scanning microscope (Germany), in order to record the surface morphology characteristics of ZnO nanoparticles. A Perkin Elmer FT-IR spectroscopy instrument

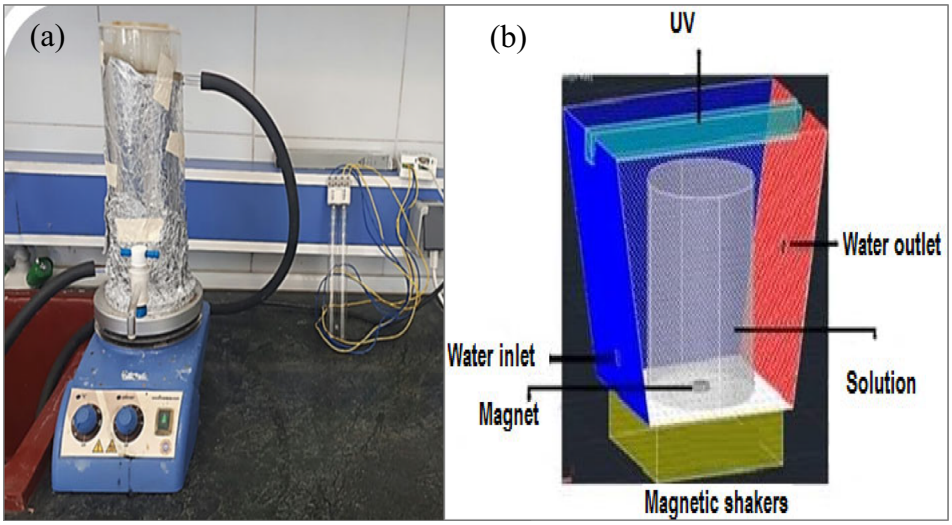

Fig. 1. Experimental set (a), and schematic diagram (b) of the photocatalytic reactor used.

(USA) was used to analyze the functional groups of samples of ZnO nanoparticles within the 500–4000 1/cm wavenumbers region. Moreover, the ZnO nanoparticles were characterized by pH of zero point of charge (pHzpc) in a manner similar to that described by [41].

2.3. Experimental work and photocatalytic reactor

The experimental work was conducted in a system of batches using a series of 500 mL flasks at the following stable conditions: 200 mL of catechol solution, laboratory temperature, agitation speed of 500 rpm. The photocatalytic reaction of catechol with ZnO nanoparticles catalyst was performed by the photochemical reactor using a UV illumination lamp (Toshiba, Japan) as depicted in Fig. 1. Additionally, the variation of the degradation efficiency of catechol was examined experimentally by using the variation of the parameters via pH (3, 7, 11), dosage of ZnO nanoparticles (0.2, 0.225, 25 g/L), initial concentration of catechol (10, 105, 200 mg/L), reaction time (15, 67.5, 120 min), and UV radiation intensity (8, 24, 48 w). At specific time intervals during each test, aliquots of 3 mL from each solution were taken, filtered, centrifuged, and then tested for the remaining catechol concentration using a UV/VIS spectrometer (T80$^+$, PG Instrument Ltd., UK). Predominantly, samples taken were analyzed in triplicate, thereby determining the average results. Furthermore, the results obtained from the effects of the reaction time were employed for the kinetic study. The percentage of degraded catechol (%*Degradation*) by the photocatalytic process was calculated using Eq. (7) [42].

$$\%Degradation = \frac{(C_o - C_t) \times 100}{C_o} \quad (7)$$

where %*Degradation* is the actual degradation efficiency of the catechol, C_0 (mg/L) and C_e (mg/L) are the initial and non-degraded concentrations of the catechol, respectively.

2.4. Statistical analysis using Box-Behnken methodology

In the current study, the Box-Behnken experimental design methodology was applied in order to investigate the effects on the degradation process, and to optimize: pH (A); dose of ZnO nanoparticles (B); initial catechol concentration (C); reaction time (D); and UV radiation (E). The employment of the Box-Behnken experimental design methodology provides a mathematical relationship between factors and the experimental results that can be fitted to a second-order polynomial model as the equation [35–37]. Consequently, Eq. (8) is suggested for developing a mathematical correlation between the degradation efficiency of catechol (%*Predicted Removal*) and the selected five independent parameters [43]. This equation is very helpful in evaluating the effects and finding the optimum values of five selected experimental parameters on the degradation efficiency of cephalexin.

$$\begin{aligned}\%Predicted\ Removal = {} & \beta_0 + \beta_1 A + \beta_2 B + \beta_3 C + \beta_4 D + \beta_5 E + \beta_6 AB \\ & + \beta_7 AC + \beta_8 AD + \beta_9 AE + \beta_{10} BC + \beta_{11} BD \\ & + \beta_{12} BE + \beta_{13} CD + \beta_{14} CE + \beta_{15} DE + \beta_{16} A^2 \\ & + \beta_{17} B^2 + \beta_{18} C^2 + \beta_{19} D^2 + \beta_{20} E^2 \end{aligned} \quad (8)$$

where β_0 is the zero-order constant; β_1 to β_{10} are the first-order main effect constants, and β_{11} to β_{20} are the second-order main effect constants of the regression equation. These constants were determined by employing the Design-Expert Software (Version VII).

Notably, the quality and goodness of the proposed model (Eq. (8)), the coefficient of determination (R^2), and adjusted coefficient of determination ($R^2_{Adjusted}$), were determined. Besides this, the normal distribution of the residuals and the plot of actual values versus predicted values, were employed. Analysis of variance (ANOVA) was applied as a method of statistical analysis of responses, where the probability critical level (*p*-value) of 0.05 was considered to reflect the statistical significance of the parameters of the proposed model. The range and levels of the factors based on experimental design are presented in Table 1.

3. Results and discussion

3.1. Characteristic of ZnO nanoparticles

Fig. 2 depicts high-resolution TEM and SEM images of a ZnO

Table 1
Variables, levels of design experiments, and Box-Behnken Design (5 factors, 10 central points, and 50 runs).

Variable	Code	Range and level		
		Low level (−1)	Central point (0)	High level (+1)
pH	A	3	7	11
ZnO nanoparticles dosage (g/L)	B	0.2	0.225	0.25
Initial catechol conc. (mg/L)	C	10	105	200
Reaction time (min)	D	15	67.5	120
UV radiation intensity (W)	E	8	24	40

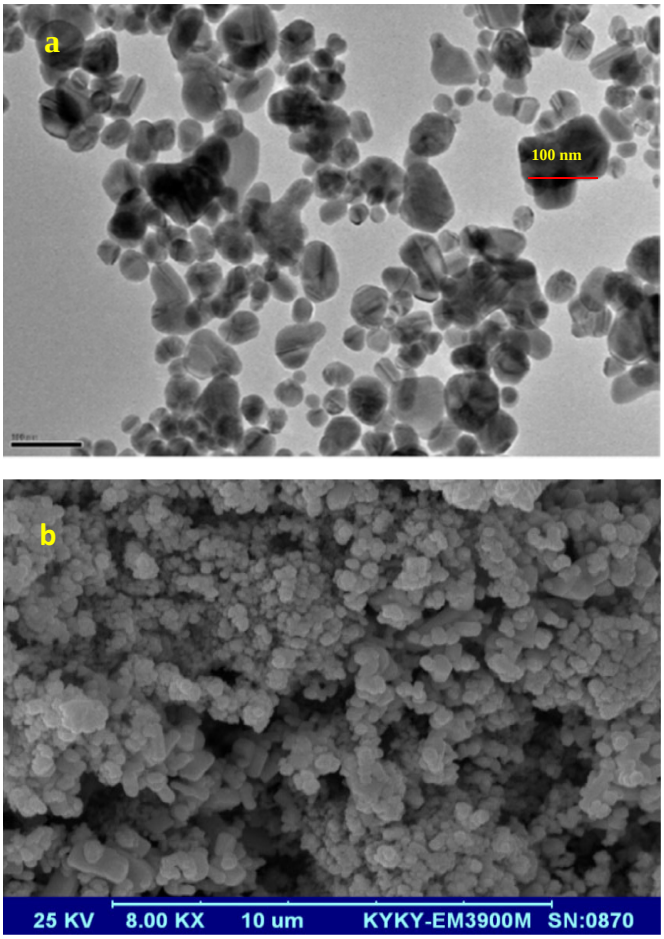

Fig. 2. TEM (a) and SEM (b) images of ZnO nanoparticles.

sample. It was apparent from the TEM image (Fig. 2a) that this material has irregularly shaped particles, nearly most of which are spherical, with an average size < 100 nm, confirming the nano size of the purchased ZnO nanoparticles. Also, this image showed that these nanoparticles are mono-dispersed and thus, their agglomeration is low. This is a positive reaction and catalytical property of ZnO nanoparticles, due to the fact that the tiny particles, after agglomeration, will lose a proportion of their surface area allocated for the reaction with molecules of the pollutants [44]. Furthermore, Fig. 2b depicts a SEM image of ZnO nanoparticles taken at 8000× magnification. Generally, the surface of these ZnO nanoparticles is coarse and consists of several non-uniform and separated grains (light color). Besides, it can be very noticeable owing to the several deep cavities formed which are dark in color. These morphological properties of the selected catalyst represent a positive feature by providing a high surface area for the pollutant molecules' adhering and reaction.

The XRD patterns of the ZnO nanoparticles are shown in Fig. 3. Generally, this pattern is necessary for gathering information about the approximate size and the crystalline structure of the solid particles. On the basis of the Scherrer equation, the average crystallite size of ZnO nanoparticles was 13 nm. The diffraction peak observed at 2θ = 31°, 34°, and 37°, represent the crystalline structure of ZnO nanoparticles with a hexagonal wurtzite phase (JCPDS:36-1451) [45]. In addition to this, the sharp peaks at 2θ = 47°, 57°, 63° and 68° confirming a high crystallinity structure of ZnO nanoparticles as well as the tested sample of ZnO nanoparticles were of a high quality [31].

The FT-IR analysis of ZnO nanoparticles is depicted in Fig. 4, which shows that the surface of the catalyst comprises several strong and active groups. The strong peaks were detected in the range of 3500–3800 cm^{-1}, which correspond to the O—H stretching mode of the hydroxyl group. The hydroxyl impurities are probably the result of the hydroscopic nature of the ZnO nanoparticles. The bands found at 2300 cm^{-1} are attributed to the presence of alkane groups (C—H stretching vibration). The peaks detected that lay in the range of 1300 to 1500 cm^{-1} belong to symmetrical and asymmetrical stretching of the zinc carboxylate groups. The weak absorption band observed in the FT-IR spectrum of ZnO nanoparticles of 667.03 cm^{-1} belongs to the stretching vibration mode of C—O groups [25,30].

3.2. Results of the statistical analysis

The Box-Behnken statistical model was applied with the detailed input values as listed in Table 2 (5 factors, 10 central points, and 50 runs). This table lists the experimental design matrix of the Box-Behnken statistical model, and the actual and predicted degradation efficiency of the catechol. Therefore, the quadratic model to predict the percentage of degradation of catechol from aqueous solution using ZnO nanoparticles as the catalyst during photocatalyst process was obtained. This model can be written as shown in Eq. (9) with five coded factors.

$$\%Predicted\ Removal = 188 - 17.7A + 11.4B - 6.2C + 5.1D + 7.1E - 0.68AB + 0.61AE + 0.03CD \quad (9)$$

Table 3 lists the results of ANOVA for the degradation efficiency of catechol using ZnO nanoparticles under the photocatalyst process. Significant parameters with p-value < 0.05 have been obtained in the present study for the input response variables, indicating that the experimental data can adequately describe the proposed model obtained by the Box-Behnken response surface methodology (Eq. (9)). Additionally, a high value of R^2 value was determined (0.950) which has a logical fit with $R^2_{\ Adjusted}$ value as determined to be equal to 0.927. Also, the validity of the model is confirmed by the insignificance of the p-value of lack-of-fit which was found to be 0.82. This value is greater than the lowest limit of fit as recommended to be (0.05) [36,46]. From another perspective, Fig. 5 graphically depicts the normal probability plot of residuals from the least-squares fitting for the response percentage of catechol degradation. This figure shows that the points on the plot lie reasonably close to a straight line as well, as the residuals follow a normal distribution pattern. Fig. 6 is a random scatter plot of the actual values (Eq. (7)), and predicted results (Eq. (9)) of the degradation efficiency of catechol. It can be seen that both the predicted and actual results are randomly scattered around the 45° straight line, which confirms that the error values between the actual and predicted values have zero mean. All these results indicate a high correlation and adequacy of the proposed model to predict the degradation process of catechol using the photocatalytic reactor with ZnO nanoparticles as a catalyst. The statistical analysis revealed that each factor in Eq. (9) is a contributing factor in this equation, but to different degrees, as visualized in Fig. 7.

3.3. Effect of experimental parameters

3.3.1. pH

The pH of an aqueous solution is one of the most important effective factors in chemical reactions in the photocatalytic process ([12]; Shukla et al., 2012). This is due to the fact that this parameter can alter the surface properties and charge of metal oxides depending on the pHpzc of the utilized catalyst. In addition to this, this parameter can have an effect on the contaminant's structure, mechanism of radical hydroxyl production, and reaction kinetics during the photocatalytic process [47,48]. Towards this end, the current study makes an attempt to ascertain the efficiency of ZnO nanoparticles in the degradation of catechol molecules at pH ranging from 3 to 11, with the variation in the dose of ZnO nanoparticles = 0.20–0.25 g/L solution (Fig. 8); and UV radiation intensity = 8–40 W (Fig. 9). The results plotted in these two

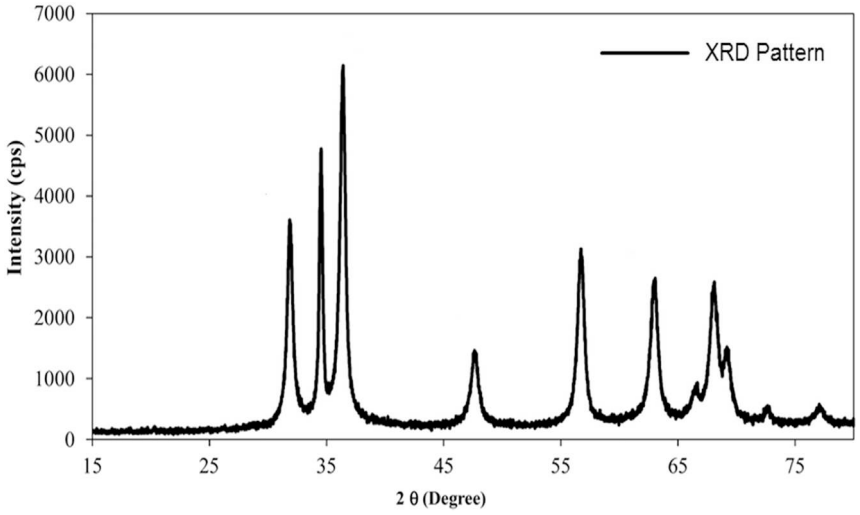

Fig. 3. The XRD pattern of ZnO nanoparticles.

figures demonstrated that the high efficiencies of catechol degradation occurred at acidic pH values and vice versa. The reason behind this phenomena is well known, that the phenolic compounds, such as catechol, have negative charges on the surface and they can be adsorbed on the surfaces of ZnO nanoparticles when the solution with pH is less than pH_{pzc}, therefore, at acidic pH, the surface charge of the catalyst and pollutant levels are non-homonymous. Moreover, at pH > 7 the electrostatic repulsion rate between the catalyst particles and the organic pollutant molecules is high, leading to a decrease in reaction rate between them; thus the decrease in degradation efficiency. On the other hand, it is well known that the photocatalytic process at the alkaline level of pH is ineffective in producing high hydroxyl radicals; also the hydrogen peroxide is rapidly decomposed by preformed hydrogen radicals into water and oxygen. Under these circumstances, the degradation rate of catechol is hampered at alkaline pH values [23,40,49].

3.3.2. Dosage of ZnO nanoparticles

As illustrated previously, the effect of the variation that the dose of the catalyst has on the removal process of the catechol was investigated within the range of 0.20–0.25 g of ZnO nanoparticles per 1 L catechol solution. The results of this experiment are plotted in Fig. 8. In fact, the dosage of the catalyst nanoparticles is another important parameter that needs to be studied, as it may have significant effects on the performance of the photocatalysts process. In addition to this, an evaluation of the optimum quantity of catalyst is one of the vital characteristics from the economic point of view. From Fig. 7, the percentage degradation of catechol increased with the increase in dosage of ZnO nanoparticles. The reason for this behavior is the increase in the amount of catalyst in the aqueous solution, which in turn increases the surface area or reaction sites. Therefore, more UV radiation will be absorbed by the catalyst particle which ultimately leads to a further increase in production of hydroxyl radicals [26]. The mechanism of this process is that in the photocatalytic reaction using ZnO nanoparticles, the surface of the catalyst absorbs UV radiation with energy greater than the energy level of the band gap and, therefore, more free electrons will be generated. Besides, the surface of the nanoparticles will have more small holes. The holes in the surfaces of ZnO nanoparticles can enhance the performance of the photocatalysis process by increasing the surface area of the reaction. Simultaneously, these generated electrons may react with H_2O and O_2 in an aqueous solution and produce $O\cdot^-$ and OH · radicals which are essential for the degradation of organic molecules (Eqs. (1)–(6)).

3.3.3. Intensity of UV radiation

The principle of the photocatalytic process is the irradiation of the catalyst utilized to UV radiation. This mechanism will offer several positive operational properties that belong to the enhancement of

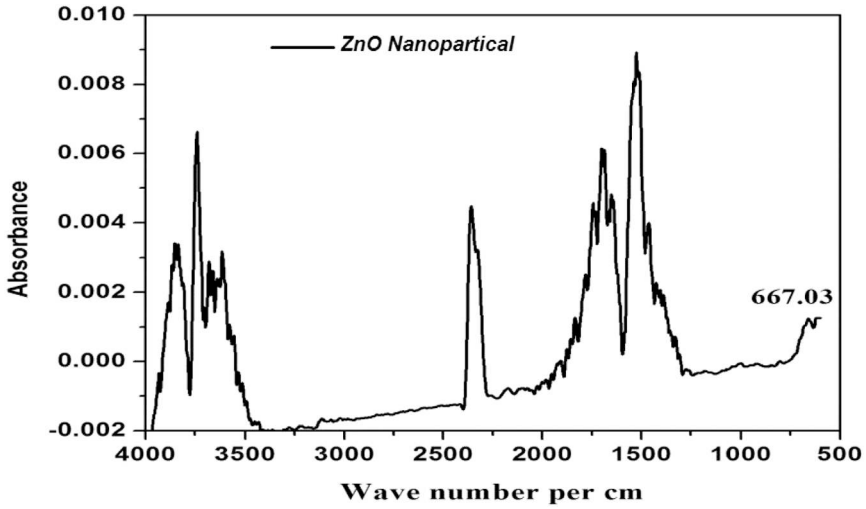

Fig. 4. FTIR spectra of the ZnO nanoparticles.

Table 2
Results of analyses of variance for the degradation efficiency of catechol using ZnO nanoparticles under photocatalyst process.

Run	A (pH)	B (ZnO dose)	C (Initial concentration)	D (Reaction time)	E: (UV intensity)	%*Degradation*
1	3	0.225	200	67.5	28	60.9
2	7	0.225	10	67.5	8	56
3	11	0.25	105	67.5	28	26
4	11	0.2	105	67.5	28	15
5	7	0.225	105	67.5	28	54.1
6	3	0.25	105	67.5	28	71.5
7	11	0.225	105	15	28	10
8	7	0.225	200	67.5	48	45.1
9	7	0.25	105	15	28	56
10	7	0.225	200	15	28	35.5
11	11	0.225	10	67.5	28	30
12	7	0.225	105	120	48	56.1
13	7	0.25	105	67.5	8	60.2
14	11	0.225	105	120	28	24.5
15	7	0.225	105	67.5	28	53.6
16	7	0.225	105	15	8	38
17	11	0.225	200	67.5	28	14.5
18	7	0.225	105	67.5	28	54.4
19	7	0.2	10	67.5	28	39
20	7	0.2	105	67.5	48	32.5
21	7	0.2	105	120	28	34.7
22	7	0.225	200	120	28	42.9
23	7	0.25	200	67.5	28	55.6
24	3	0.2	105	67.5	28	52
25	3	0.225	10	67.5	28	69.4
26	7	0.2	200	67.5	28	28.2
27	3	0.225	105	67.5	8	66.5
28	3	0.225	105	67.5	48	67.8
29	7	0.225	105	67.5	28	52.7
30	7	0.225	105	67.5	28	51.9
31	11	0.225	105	67.5	48	22
32	7	0.225	10	15	28	54.1
33	7	0.225	105	67.5	28	53.5
34	7	0.225	200	67.5	8	34
35	7	0.25	105	67.5	48	61.8
36	7	0.225	105	120	8	54
37	3	0.225	105	15	28	56.7
38	3	0.225	105	120	28	65.1
39	7	0.2	105	67.5	8	29.9
40	7	0.225	105	67.5	28	51.8
41	7	0.225	105	15	48	44.2
42	7	0.225	10	67.5	48	60.1
43	7	0.225	10	120	28	59.9
44	7	0.2	105	15	28	26.6
45	11	0.225	105	67.5	8	15
46	7	0.225	105	67.5	28	52.4
47	7	0.25	105	120	28	62.1
48	7	0.25	10	67.5	28	64.2
49	7	0.225	105	67.5	28	50.9
50	7	0.225	105	67.5	28	52

radical hydroxyl production, and an increase in the number of cavities at the surface of the catalyst particles that will result in an increase in the surface area of the reaction. The effect of the UV radiation in the photocatalytic reactor was examined using UV lamps of intensity of 8, 24, and 48 W, and the results are depicted in Fig. 9. It is obvious that the increase in the intensity of UV radiation led to the linear increase in the degradation efficiency of catechol owing to the above mentioned reasons. The results obtained from this experimental work are similar to those derived by Abramović et al. [24], who concluded that the degradation of the herbicide, clomazone, was hastened with the increase in the intensity of UV radiation during the photocatalytic reaction with TiO_2 nanoparticles as catalyst.

3.3.4. Initial catechol concentration

The initial effect of catechol concentration on the degradation of its efficiency using ZnO nanoparticles catalyst was tested further in the present study. The test was as a function of different initial concentrations, i.e., 10, 105, and 200 mg/L, and the reaction time from 15 to 120 min (Fig. 10). The results indicated that the increase in catechol concentration from 10 to 105 mg/L has none or little effect on its degradation efficiency. With further increase in catechol concentration from 105 to 200 mg/L, the degradation efficiency decreased abruptly. The overall observation can be ascribed to the availability of the high number of non-reacted sites that can cover the degradation of catechol at lower concentrations such as below 105 mg/L. Subsequently, with a further increase in the concentration of the pollutant to above 105 mg/L, the occupying or reaction of most of the catalyst nanoparticles was behind the reason for depletion in the percentage of degradation. This can be attributed to the increase in the concentration of the pollutant which can increase the competition of hydroxyl radicals that are essential for the degradation of the pollutant molecules [50]. On the other hand, the presence of byproduct chemicals due to the decomposition of catechol at high concentrations can lead to the consumption of additional radical hydroxyls and, in turn, reduces the removal efficiency of catechol. Similar results were obtained by another study conducted by Shukla et al. [51] and Asadgol et al. [28].

Table 3
Analyses of variance for a quadratic model removal of catechol.

Model	Sum of squares	Mean square	F-value	p-Value
Theoretical model (Eq. (9))	14,667	958	1106	< 0.0001
A	7487	7487	95.2	< 0.0001
B	86.17	86.17	321.2	< 0.0001
C	278.3	278.3	378.5	0.009
D	347.6	347.6	296.8	0.02
E	230.3	230.3	914.8	0.0054
$A)^2$)	840	840	859	< 0.0001
$B)^2$)	106	106	195.4	< 0.0001
$C)^2$)	3730	3730	4567	0.01
$D)^2$)	955	955	1281	0.025
$E)^2$)	702	702	833.2	0.039
A*B	74	74	89.8	0.001
A*E	26.8	26.8	36.12	0.025
C*D	71	71	80.2	0.041
Residual	21.64	0.85	–	–
Lack of Fit	21.39	0.79	0.58	0.82
Pure Error	11.25	1.25	–	–
Cor Total	14,997	–	–	–

$R^2 = 0.951$. $R^2_{Adjusted} = 0.927$.

3.3.5. Reaction time

The effects of the variation in reaction time on the degradation efficiency were examined within 15–120 min, and the results are presented in Fig. 10. However, the degradation performance of ZnO nanoparticles in the photocatalytic reaction was fast. It can be seen that an increase in the agitation time above 15 min, imparted a noticeable effect on the removal efficiency of catechol, and relatively 45% degradation efficiency was achieved with the first 15 min of reaction time (10 mg/L initial concentration). Indeed, this behavior of fast reaction process imparts a positive property to the catalyst material which, in turn, makes it an excellent material for practical applications in photocatalytic treatment units [34,52]. Subsequently, the degradation efficiency was increased to 56% with an increase in reaction time to 120 min. The occurrence of this phenomenon can be attributed to the available and adequate time to produce more free radical hydroxyl concentration, thereby, these radicals will degrade more catechol molecules, and thus, the degradation efficiency was increased [53–55]. This finding is similar to that obtained in the degradation of other organic pollutants [52,56].

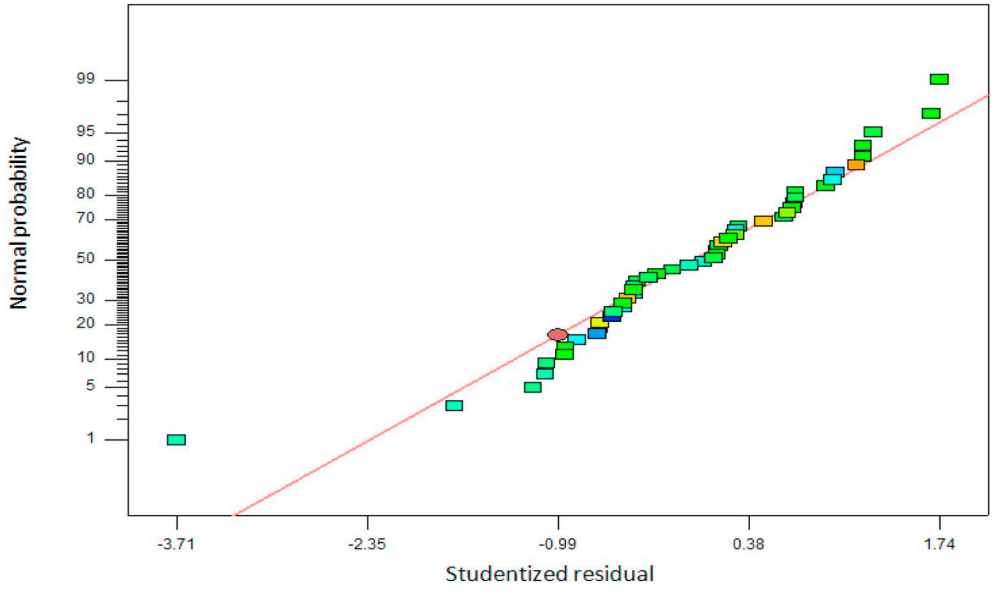

Fig. 5. Normal probability plot of residuals obtained by ANOVA for degradation of catechol using the ZnO nanoparticles catalyst.

3.4. Optimization of the experimental parameters

The aim of conducting the optimization process is to find a combination of experimental variable levels in which the removal of catechol reaches its maximum value. In order to achieve this aim, the Box-Behnken design methodology is applied as an efficient tool to predict the best operating mode between the ranges of studied experimental variables. The results highlighted that the proposed model predicted about 69.8% of catechol removal under optimal conditions including: pH = 3; a dose of ZnO nanoparticles = 0.24 g/L; reaction time = 98 min; initial concentration of catechol = 74 mg/L; and UV radiation intensity = 40 W. The factor of desirability was 0.96 which represents a completely desirable, or ideal response value of these conditions [57] (Fig. 11).

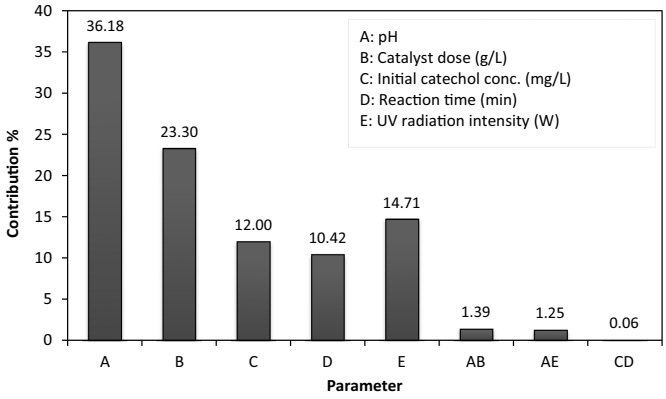

Fig. 7. The percentage contribution of the parameters of the proposed model (Eq. (9)).

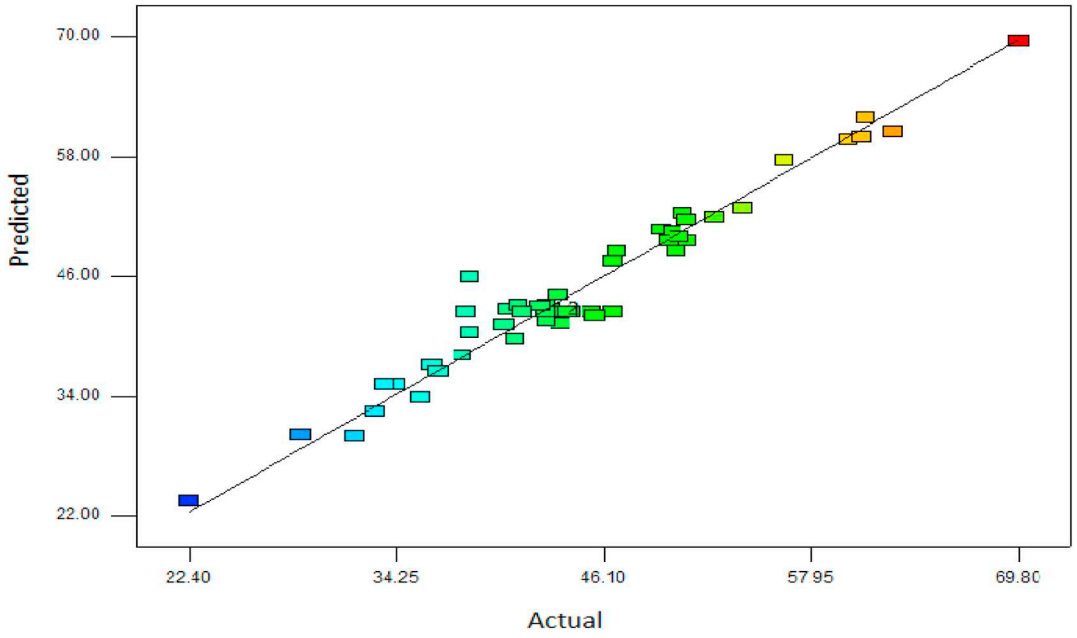

Fig. 6. Correlations between the experiments with predicted values of catechol removal efficiency.

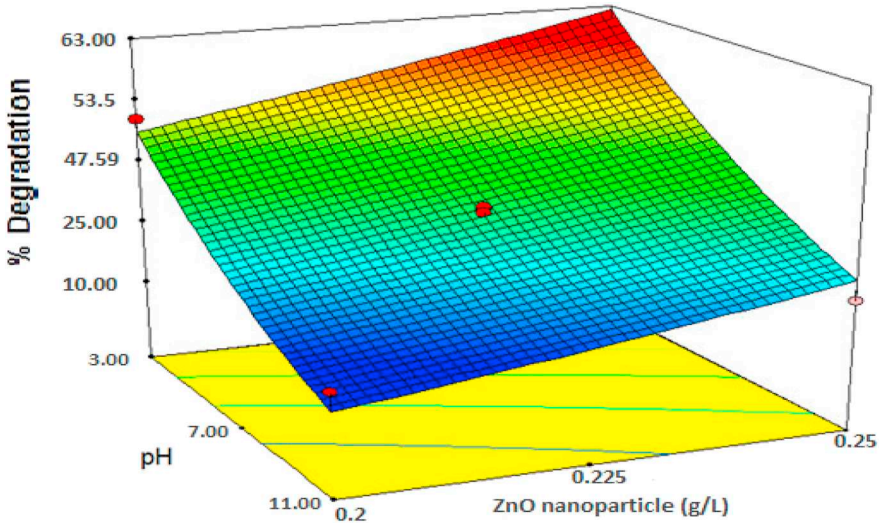

Fig. 8. Degradation efficiency of catechol as a function of pH and ZnO nanoparticles dose.

3.5. Kinetic degradation mechanism

In the chemical reaction, the experimental kinetics should be investigated in order to identify the mechanism of pollutants' degradation. Furthermore, it is essential to make use of the reaction rate kinetics for investigating the catalytic performance for removal of catechol. In the present study, the Langmuir-Hinshelwood (Eq. (10)) was used for modeling the experimental kinetic data.

This formalism is mostly used for modeling experimental data, and for the description of the kinetic degradation systems of organic materials [60,61].

$$r_0 = -\frac{dC}{dt} = K'\left(\frac{K\,C_o}{1 + KC_0}\right) \tag{10}$$

where r_0; K', and K are the oxidation reaction rate (mg/L min); the constant of reaction rate (mg/L min); and the uptake of coefficient of pollutant (catechol) (L/mg), respectively.

In case of very low pollutant concentration ($K \ll 1$), Eq. (10) can be written as follows:

$$-\frac{dC}{dt} = k_{obs} \tag{11}$$

$$\ln\left(\frac{C}{C_0}\right) = -k_{obs}t \tag{12}$$

where k_{obs} is the rate constant of the first-order model (min^{-1}), and t is the reaction time (min).

The linear analysis results of this model with the experimental data of catechol degradation are reported in Table 4. It reveals that the experimental data are in good agreement with the Langmuir-Hinshelwood model, which is further confirmed by satisfactorily high R^2 values. The model parameter of reaction rate (k_{obs}) is determined from the linear plot of $\ln\left(\frac{C_t}{C_o}\right)$ versus time (Table 4). The high K_{obs} values were determined at the studied range of catechol concentrations, indicating a high rate of photocatalytic reaction at these values [58,59].

4. Conclusion

In the present study, we have investigated ZnO nanoparticles as a catalyst for the photocatalytic degradation of catechol from wastewater under different experimental parameters. The characterization, using specific diagnostic techniques, demonstrated that the prepared catalyst of ZnO nanoparticles have good catalytical properties like high surface

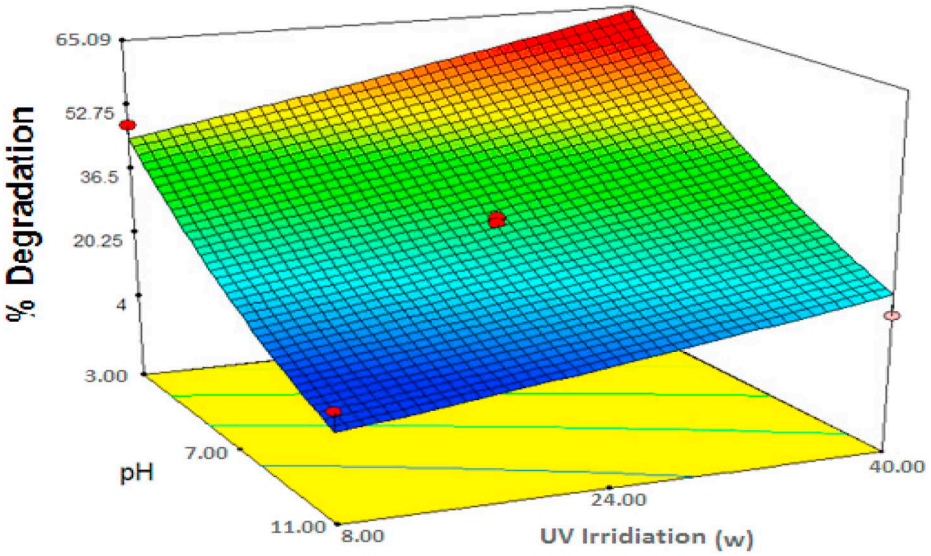

Fig. 9. Degradation efficiency of catechol as a function of pH and intensity of UV radiation.

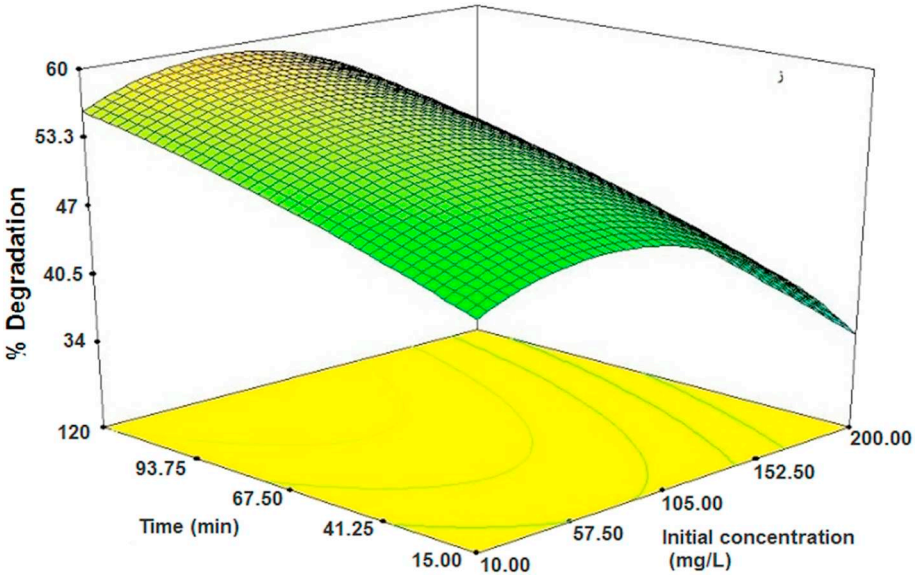

Fig. 10. Degradation efficiency of catechol as a function of reaction time and initial catechol concentration.

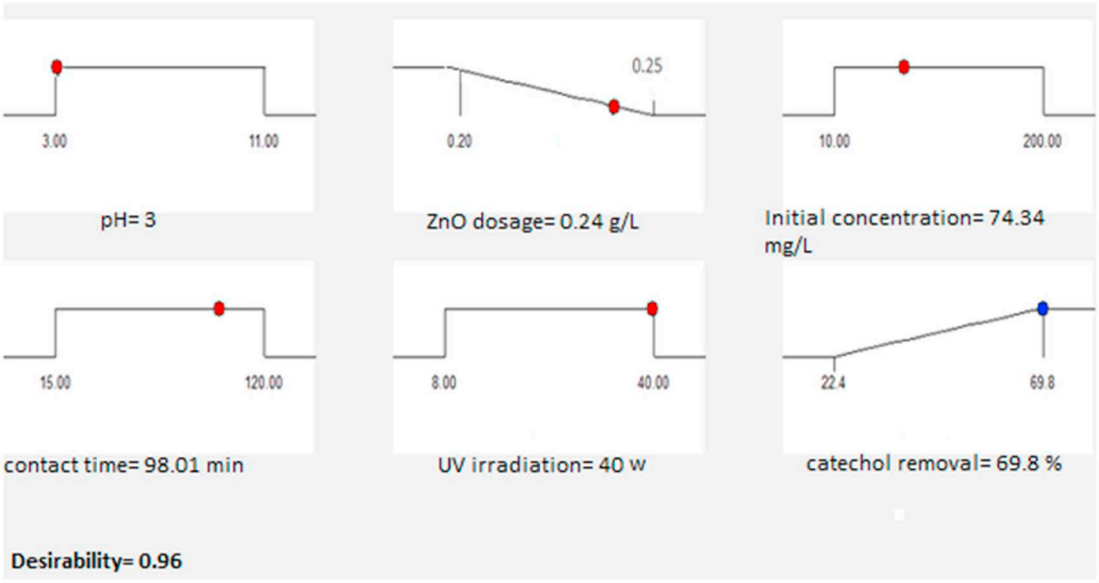

Fig. 11. Optimum conditions designed using the Box-Behnken statistical method.

Table 4
The calculated parameters of the Langmuir-Hinshelwood model at different environmental conditions.

Parameter	Value	Kinetic equation ($Y = \ln\left(\frac{C}{C_0}\right)$ and $x = t$)	k_{obs} (min^{-1}) × 10^3	R^2
pH	3	*Y = 0.0081x + 0.76*	8.1	0.979
	7	*Y = 0.00057x + 0.616*	5.5	0.963
	11	*Y = 0.00049x + 0.053*	4.9	0.936
ZnO nanoparticles dosage (g/L)	0.2	*Y = 0.0034x + 0.43*	2.7	0.946
	0.225	*Y = 0.0027x + 0.3*	3.4	0.969
	0.25	*Y = 0.025x + 1.08*	25	0.989
Initial concentration (mg/L)	10	*Y = 0.0181x + 1.004*	18.1	0.997
	105	*Y = 0.0138x + 0.13*	13.8	0.991
	200	*Y = 0.0116x + 0.778*	11.6	0.966
UV radiation intensity (W)	8	*Y = 0.0086x + 0.69*	8.6	0.979
	24	*Y = 0.2569x + 0.821*	25	0.998
	40	*Y = 0.099x + 1.67*	45	0.965

area, strong functional groups, high pore size, and nano-sized range of particle diameter. According to the results of the statistical analysis utilizing the Box-Behnken statistical methodology, the proposed quadratic model was successful in predicting the degradation process of catechol, and all the parameters studied had statistically significant probability critical levels. Further, the catechol degradation efficiency reached 69% under conditions such as: pH = 3; initial catechol concentration = 74 mg/L; ZnO nanoparticles dosage = 0.24 g/L; reaction time = 98 min; and under exposure to UV radiation of 40 W. The results of the optimization process showed that the experimental parameters that were studied played a role in contributing towards the degradation process with a different trend, but they can also be ranked as pH > catalyst dose > UV radiation intensity > initial catechol concentration > reaction time. The kinetic degradation data followed the Langmuir-Hinshelwood model because this model had statistically significant parameters. These results suggest that the ZnO nanoparticles were an attractive and effective catalyst for the degradation of catechol in the photocatalytic treatment systems. In future studies, the intermediate compounds that were generated during the photocatalytic degradation of catechol should also be considered.

Acknowledgements

The authors appreciate than Research and Technology of Birjand and Zahedan University of Medical Sciences for supporting and funding of this study. Tariq J. Al-Musawi is also thankful to Isra University for the support extended for this work.

References

[1] M. Ferreira, M. Pinto, I.C. Neves, A. Fonseca, O. Soares, J. Órfão, M.F.R. Pereira, J.L. Figueiredo, P. Parpot, Electrochemical oxidation of aniline at mono and bimetallic electrocatalysts supported on carbon nanotubes, Chem. Eng. J. 260 (2015) 309–315.
[2] A.A. Gürten, S. Ucan, M.A. Özler, A. Ayar, Removal of aniline from aqueous solution by PVC-CDAE ligand-exchanger, J. Hazard. Mater. 120 (2005) 81–87.
[3] W.A. Khanday, B.H. Hameed, Zeolite-hydroxyapatite-activated oil palm ash composite for antibiotic tetracycline adsorption, Fuel 215 (2018) 499–505.
[4] M.M. Soori, E. Ghahramani, H. Kazemian, T.J. Al-Musawi, M. Zarrabi, Intercalation of tetracycline in nano sheet layered double hydroxide: an insight into UV/VIS spectra analysis, J. Taiwan Inst. Chem. Eng. 63 (2016) (2016) 271–285.
[5] W.A. Khanday, M. Asif, B.H. Hameed, Cross-linked beads of activated oil palm ash zeolite/chitosan composite as a bio-adsorbent for the removal of methylene blue and acid blue 29 dyes, Int. J. Biol. Macromol. 95 (2017) 895–902.
[6] M.N. Sepehr, T.J. Al-Musawi, E. Chahramani, H. Kazemian, M. Zarrabi, Adsorption performance of magnesium/aluminum layered double hydroxide nanoparticles for metronidazole from aqueous solution, Arab. J. Chem. 10 (2017) 611–623.
[7] M.S. Gasser, H.T. Mohsen, H.F. Aly, Humic acid adsorption onto Mg/Fe layered double hydroxide, Colloids Surf. A Physicochem. Eng. Asp. 331 (2008) 195–201.
[8] S.C. Low, C. Liping, L.S. Hee, Water softening using a generic low cost nano-filtration membrane, Desalination 221 (1) (2008) 168–173.
[9] S. Liu, M. Lim, R. Fabris, C. Chow, K. Chiang, M. Drikas, et al., Removal of humic acid using TiO2 photocatalytic process–fractionation and molecular weight characterisation studies, Chemosphere 72 (2) (2008) 263–271.
[10] J. Anotai, C.-C. Su, Y.-C. Tsai, M.C. Lu, Effect of hydrogen peroxide on aniline oxidation by electro-Fenton and fluidized-bed Fenton processes, J. Hazard. Mater. 183 (2010) 888–893.
[11] S.A. El-Safty, A. Shahat, M. Ismael, Mesoporous aluminosilica monoliths for the adsorptive removal of small organic pollutants, J. Hazard. Mater. 201 (2012) 23–32.
[12] A.D. Shiraz, A. Takdastan, S.M. Borghei, Photo-Fenton like degradation of catechol using persulfate activated by UV and ferrous ions: influencing operational parameters and feasibility studies, J. Mol. Liq. 249 (2018) 463–469.
[13] A.A. Aghapour, G. Moussavi, K. Yaghmaeian, Degradation and COD removal of catechol in wastewater using the catalytic ozonation process combined with the cyclic rotating-bed biological reactor, J. Environ. Manag. 157 (2015) 262–266.
[14] S. Chen, D. Sun, J.-S. Chung, Simultaneous methanogenesis and denitrification of aniline wastewater by using anaerobic–aerobic biofilm system with recirculation, J. Hazard. Mater. 169 (2009) 575–580.
[15] J. DeZuane, Handbook of Drinking Water Quality, John Wiley & Sons, 1997.
[16] A.H. Mahvi, A. Maleki, M. Alimohamadi, A. Ghasri, Photo-oxidation of phenol in aqueous solution: toxicity of intermediates, Korean J. Chem. Eng. 24 (1) (2007) 79–82.
[17] K. Shakir, H. Ghoneimy, A. Elkafrawy, S.G. Beheir, M. Refaat, Removal of catechol from aqueous solutions by adsorption onto organophilic-bentonite, J. Hazard. Mater. 150 (2008) 765–773.
[18] R. Subramanyam, I. Mishra, Biodegradation of catechol (2-hydroxy phenol) bearing wastewater in an UASB reactor, Chemosphere 69 (2007) 816–824.
[19] W.A. Khanday, F. Marrakchi, M. Asif, B.H. Hameed, Mesoporous zeolite–activated carbon composite from oil palm ash as an effective adsorbent for methylene blue, J. Taiwan Inst. Chem. Eng. 0 (2016) 1–10.
[20] Z. Li, Y. Huang, H. Wang, D. Wang, X. Wang, F. Han, Three-dimensional hierarchical structures of ZnO nanorods as a structure adsorbent for water treatment, J. Mater. Sci. Technol. 33 (2017) 864–868.
[21] W.A. Khanday, B.H. Hameed, Catalytic pyrolysis of oil palm mesocarp fibre on a zeolite derived from low-cost oil palm ash, Energy Convers. Manag. 127 (2016) 265–272.
[22] M.A. Zazouli, D. Balarak, Y. Mahdavi, Pyrocatechol removal from aqueous solutions by using Azolla filiculoides, Health Scope 2 (2013) 25–30.
[23] M.A. Zazouli, M. Taghavi, Phenol removal from aqueous solutions by electrocoagulation technology using iron electrodes: effect of some variables, J. Water Resour. Prot. 4 (2012) 980–983.
[24] B.F. Abramović, V.N. Despotović, D.V. Šojić, D.Z. Orčić, J.J. Csanádi, D.D. Četojević-Simin, Photocatalytic degradation of the herbicide clomazone in natural water using TiO2: kinetics, mechanism, and toxicity of degradation products, Chemosphere 93 (2013) 166–171.
[25] M. El-Kemary, H. El-Shamy, I. El-Mehasseb, Photocatalytic degradation of ciprofloxacin drug in water using ZnO nanoparticles, J. Lumin. 130 (2010) 2327–2331.
[26] U.I. Gaya, A.H. Abdullah, Z. Zainal, M.Z. Hussein, Photocatalytic treatment of 4-chlorophenol in aqueous ZnO suspensions: intermediates, influence of dosage and inorganic anions, J. Hazard. Mater. 168 (2009) 57–63.
[27] C. Hariharan, Photocatalytic degradation of organic contaminants in water by ZnO nanoparticles: revisited, Appl. Catal. A Gen. 304 (2006) 55–61.
[28] Z. Asadgol, H. Forootanfar, S. Rezaei, A.H. Mahvi, M.A. Faramarzi, Removal of phenol and bisphenol-A catalyzed by laccase in aqueous solution, Journal of Environmental Health Science & Engineering 12, 93, DOI, 2014. http://www.ijehse.com/content/12/1/93.
[29] W.A. Khanday, P.U. Okoye, B.H. Hameed, Biodiesel byproduct glycerol upgrading to glycerol carbonate over lithium–oil palm ash zeolite, Energy Convers. Manag. 151 (2017) 472–480.
[30] S.B. Rana, V.K. Bhardwaj, S. Singh, A. Singh, N. Kaur, Influence of surface modification by 2-aminothiophenol on optoelectronics properties of ZnO nanoparticles, J. Exp. Nanosci. 1–15 (2012).
[31] R. Yogamalar, R. Srinivasan, A. Vinu, K. Ariga, A.C. Bose, X-ray peak broadening analysis in ZnO nanoparticles, Solid State Commun. 149 (2009) 1919–1923.
[32] R. Joshi, Facile photochemical synthesis of ZnO nanoparticles in aqueous solution without capping agents, Materialia 2 (2018) 104–110.
[33] L. Wang, C. Han, M.N. Nadagouda, D.D. Dionysiou, An innovative zinc oxide-coated zeolite adsorbent for removal of humic acid, J. Hazard. Mater. 313 (2016) 283–290.
[34] S.K. Kansal, M. Singh, D. Sud, Parametric optimization of photocatalytic degradation of catechol in aqueous solutions by response surface methodology, Indian J. Chem. Technol. 14 (2007) 145–153.
[35] M. Danish, W.A. Khanday, R. Hashim, N.S.B. Sulaiman, M.N. Akhtar, M. Nizam, 2017, Application of optimized large surface area date stone (Phoenix dactylifera) activated carbon for rhodamin B removal from aqueous solution: Box-Behnken design approach, Ecotoxicol. Environ. Saf. 139 (2017) 280–290.
[36] E.M. Kalhori, E. Ghahramani, T.J. Al-Musawi, H.N. Saleh, M.N. Sepehr, M. Zarrabi, Effective reduction of metronidazole over the cryptomelane-type manganese oxide octahedral molecular sieve (K-OMS-2) catalyst: facile synthesis, experimental design and modeling, statistical analysis, and identification of by-products, Environ. Sci. Pollut. Res. 25 (2018) 34164–34180.
[37] M.H. Dehghani, M. Faraji, A. Mohammadi, H. Kamani, Optimization of fluoride adsorption onto natural and modified pumice using response surface methodology: isotherm, kinetic and thermodynamic studies, Korean J. Chem. Eng. 34 (2) (2017) 454–462.
[38] M. Jain, V.K. Garg, V.K. Kadirvelu, Investigation of Cr(VI) adsorption onto chemically treated Helianthus annuus: optimization using response surface methodology, Bioresour. Technol. 102 (2011) 600–605.
[39] S. Zainal, K.Z. Nadzirah, A. Noriham, I. Normah, Optimisation of beef tenderisation treated with bromelain using response surface methodology (RSM), Agric. Sci. 4 (2013) 65–72.
[40] A. Maleki, A.H. Mahvi, A. Mesdaghinia, K. Naddafi, Degradation and toxicity reduction of phenol by ultrasound waves, Bull. Chem. Soc. Ethiop. 21 (1) (2007) 33–38.
[41] A. Mohseni-Bandpi, T.J. Al-Musawi, E. Ghahramani, M. Zarrabi, S. Mohebi, S.A. Vahed, Improvement of zeolite adsorption capacity for cephalexin by coating with magnetic Fe_3O_4 nanoparticles, J. Mol. Liq. 218 (2016) 615–624.
[42] C.-H. Weng, Y.-T. Lin, H.-M. Yuan, Rapid decoloration of Reactive Black 5 by an advanced Fenton process in conjunction with ultrasound, Sep. Purif. Technol. 117 (2013) 75–82.
[43] S. Sadaf, H.N. Bhattia, M. Arifb, M. Amina, F. Nazarc, M. Sultand, Box–Behnken design optimization for the removal of Direct Violet 51 dye from aqueous solution using lignocellulosic waste, Desalin. Water Treat. 56 (9) (2015) 2425–2437.
[44] Z.X. Chen, X.Y. Jin, Z. Chen, M. Megharaj, R. Naidu, Removal of methyl orange from aqueous solution using bentonite-supported nanoscale zero-valent iron, J. Colloid Interface Sci. 363 (2011) 601–607.
[45] A.K. Zak, W.A. Majid, M.E. Abrishami, R. Yousefi, X-ray analysis of ZnO nanoparticles by Williamson–Hall and size–strain plot methods, Solid State Sci. 13 (2011) 251–256.
[46] T. Shojaeimehr, F. Rahimpour, M.A. Khadivi, M. Sadeghi, A modeling study by response surface methodology (RSM) and artificial neural network (ANN) on Cu2+ adsorption optimization using light expended clay aggregate (LECA), J. Ind. Eng.

Chem. 20 (2014) 870–880.
[47] A.A. Mohammed, I.S. Samaka, F. Brouers, T.J. Al-Musawi, Role of Fe_3O_4 magnetite nanoparticles used to coat bentonite in zinc(II) ions sequestration, Environ. Nanotechnol. Monit. Manag. 10 (2018) 17–27.
[48] G. Safari, M. Hoseini, M. Seyedsalehi, H. Kamani, J. Jaafari, A. Mahvi, Photocatalytic degradation of tetracycline using nanosized titanium dioxide in aqueous solution, Int. J. Environ. Sci. Technol. 12 (2015) 603–616.
[49] H. Dewidar, S.A. Nosier, A.H. El-Shazly, Photocatalytic degradation of phenol solution using zinc oxide/UV, J. Chem. Health Saf. 25 (2018) 2–11.
[50] C. Ozdemir, M.K. Öden, S. Şahinkaya, E. Kalipçi, Color removal from synthetic textile wastewater by Sono-Fenton process, Clean: Soil, Air, Water 39 (2011) 60–67.
[51] P.R. Shukla, S. Wang, H.M. Ang, M.O. Tadé, Photocatalytic oxidation of phenolic compounds using zinc oxide and sulphate radicals under artificial solar light, Sep. Purif. Technol. 70 (2010) 338–344.
[52] C. Wang, C. Liu, Decontamination of alachlor herbicide wastewater by a continuous dosing mode ultrasound/Fe2+/H2O2 process, J. Environ. Sci. 26 (2014) 1332–1339.
[53] R. Alnaizy, A. Akgerman, Advanced oxidation of phenolic compounds, Adv. Environ. Res. 4 (2000) 233–244.
[54] K. Ninomiya, H. Takamatsu, A. Onishi, K. Takahashi, N. Shimizu, Sonocatalytic–Fenton reaction for enhanced OH radical generation and its application to lignin degradation, Ultrason. Sonochem. 20 (2013) 1092–1097.
[55] L. Zhou, M. Zhou, C. Zhang, Y. Jiang, Z. Bi, J. Yang, Electro-Fenton degradation of p-nitrophenol using the anodized graphite felts, Chem. Eng. J. 233 (2013) 185–192.
[56] H. Lin, H. Zhang, X. Wang, L. Wang, J. Wu, Electro-Fenton removal of Orange II in a divided cell: reaction mechanism, degradation pathway and toxicity evolution, Sep. Purif. Technol. 122 (2014) 533–540.
[57] C.D. Pimenta, M.B. Silva, R.L. Campos, W.R. Junior, Desirability and design of experiments applied to the optimization of the reduction of decarburization of the process heat treatment for steel wire SAE 51B35, Am. J. Theor. Appl. Stat. 7 (1) (2018) 35–44.
[58] M. Behnajady, N. Modirshahla, R. Hamzavi, Kinetic study on photocatalytic degradation of CI Acid Yellow 23 by ZnO photocatalyst, J. Hazard. Mater. 133 (2006) 226–232.
[59] S.B. Kim, S.C. Hong, Kinetic study for photocatalytic degradation of volatile organic compounds in air using thin film TiO_2 photocatalyst, Appl. Catal. B Environ. 35 (2002) 305–315.
[60] P. Pascariu, M. Homocianu, C. Cojocaru, P. Samoila, A. Airinei, M. Suchea, Preparation of La doped ZnO ceramic nanostructures by electrospinning–calcination method: effect of La3+ doping on optical and photocatalytic properties, Appl. Surf. Sci. 476 (2019) 16–27.
[61] P. Samoila, C. Cojocaru, L. Sacarescu, P.P. Dorneanu, A.-A. Domocos, A. Rotaru, Remarkable catalytic properties of rare-earth doped nickel ferrites synthesized by sol-gel auto-combustion with maleic acid as fuel for CWPO of dyes, Appl. Catal. Environ. 202 (2017) 21–32.